CORRESPONDENCE

Comments on "What Is the Predictability Limit of Midlatitude Weather?"

NEDJELJKA ŽAGAR

Meteorological Institute, Center for Earth System Research and Sustainability, Universität Hamburg, Hamburg, Germany

ISTVAN SZUNYOGH

Department of Atmospheric Sciences, Texas A&M University, College Station, Texas

(Manuscript received 14 June 2019, in final form 20 December 2019)

1. Introduction

Zhang et al. (2019, hereafter Zetal2019) investigated the gap between the inherent and current-day practical limit of midlatitude weather predictability by perfect model experiments. Their methodology and conclusions raise a number of questions, which we summarize as follows: 1) the experiments of Zetal2019 do not provide realistic simulations of either the current-day operational, or the future ideal evolution of the forecast errors; 2) estimates of the extension of the practical predictability by reduction of the magnitude of the initial condition uncertainty can be obtained at a much lower cost from simple parametric models of the error growth in operational forecasts; and 3) tropical-to-extratropical uncertainly propagation and other dynamical processes that can affect error growth at the large scales and left completely out of discussion by Zetal2019 are likely to play a major role in setting the limits of predictability in the midlatitudes.

In the following sections, we review the relevant literature and provide some new computational results to support the aforementioned arguments, and then conclude with some remarks on the potentials for future operational forecast improvements.

Denotes content that is immediately available upon publication as open access.

Corresponding author: Nedjeljka Žagar, nedjeljka.zagar@uni-hamburg.de

2. Representation of the analysis and forecast uncertainties

Zetal2019 generated two ensembles of forecasts to simulate the growth of forecast uncertainty for two case studies (for an NH winter and summer case), with the ECMWF operational forecast model, cycle 41r2. The model was run for 10 ensemble members of the operational ensemble of 4DVar analyses (EDA; Bonavita et al. 2012), and the ensemble variance was used as a proxy of the mean-square forecast error to estimate the current-day predictability by a numerical weather prediction (NWP) model. The second ensemble of forecasts (denoted EDA0.1) started from the same analyses after a rescaling of the analysis perturbations by a factor of 10. Zetal2019 considered the EDA perturbations to "represent the current realistic initial-condition uncertainties by the best-performing global NWP model" whereas they considered the EDA0.1 experiment representative for the evolution of the forecast uncertainty for nearly perfect initial conditions. Based on the results for the 500-hPa winds and geopotential height in the midlatitudes, Zetal2019 argued that reducing the analysis uncertainty alone could extend the midlatitude practical predictability from about 10 to 15 days.

In reality, the operational ECMWF ensemble prediction system (ENS) has to supplement the EDA initial-condition perturbations with singular vector initial-condition perturbations and a parameterization of the effect of model errors to realistically simulate the evolution of the forecast uncertainty

DOI: 10.1175/JAS-D-19-0166.1

(Isaksen et al. 2010; Leutbecher et al. 2017; Haiden et al. 2018; Lock et al. 2019). The ensemble forecast benefits of including the singular vector perturbations and a parameterization of the effect of model errors indicate that either the EDA perturbations cannot fully represent the growing initial-condition uncertainties, or the model cannot capture all processes that contribute to the growth of the forecast uncertainty. The results of Herrera et al. (2016) and Loeser et al. (2017) showed that even with these features included, the operational ECMWF ensemble was deficient in representing the forecast uncertainty in the extratropics until about the end of the second forecast day. We understand that Zetal2019 did not include the singular vector perturbations in the ensemble, because they wanted to observe the process of forecast uncertainty growth without the influence of the unique dynamics of singular vectors (e.g., Hoskins et al. 2000). However, including only a subset of the EDA perturbations and not including the singular vector perturbations and the parameterization of the effect of model errors may have hampered the ability of the ensemble to fully capture the evolution of the forecast uncertainty realistically for an extended forecast time.

The EDA method relies on the assimilation of perturbed observations to generate an ensemble of analyses to represent the probability distribution of the initial state of the atmosphere (Bonavita et al. 2012). One notable property of the resulting estimate of the analysis uncertainty is its large amplitude in the tropics, in particular, in the upper troposphere (Žagar et al. 2013; Cardinali et al. 2014; Žagar et al. 2015; Žagar 2017). Figures 6–8 of Zetal2019 show that the EDA perturbations in the midlatitudes at 500 hPa also have the largest magnitudes at zonal wavelengths larger than 1000 km. Rescaling the EDA perturbations by a constant factor reduces the magnitude of the perturbations, in the absolute sense, more drastically at the scales and in the regions where they are larger: in the tropics and at the larger scales. Hence, reduced initial-condition uncertainties in the tropics and at the large scales must have played a major role in the increased predictability in the midlatitudes in the experiments of Zetal2019.

Zetal2019 identified the rapid upscale cascade of the forecast uncertainty at the small scales as a main source of the initial error growth. One diagnostic tool they used to study the error growth process was the three-parameter model of Dalcher and Kalnay (1987). They stated that the β term "represents the error growth rate induced by the intrinsic upscale error propagation such as from small-scale moist processes."[1] First, we note that Žagar et al. (2017) carried out a scale-dependent investigation of the α and β terms and were the first to extend the standard interpretation of β, as the term that captures the effect of model errors, by showing that β also represented a rapid growth of errors toward saturation at the small scales. Second, the "super-exponential" growth in the EDA0.1 experiment discussed by Zetal2019 is a general property of the growth of very-small-magnitude initial-condition perturbations in experiments with primitive equations models (e.g., Harlim et al. 2005). The fact that low-resolution model experiments produce essentially the same super-exponential growth as the EDA0.1 experiment suggests that the high resolution of the experiment by Zetal2019 was not a key factor in the rapid growth shown in the lower panels of their Figs. 3 and 4.

3. Scale-dependent estimates of practical predictability by a parametric model

Using large samples of operational forecasts and analyses, many studies have provided estimates of the error doubling time and the limit of practical predictability for operational NWP models (e.g., Simmons and Hollingsworth 2002; Magnusson and Kallen 2013; Herrera et al. 2016). In what follows, we discuss the growth of the forecast uncertainty at several scales under the assumption that the operational 50-member ECMWF ENS can accurately estimate the magnitude of the analysis and forecast uncertainty. We use ENS data from May 2015 and June 2018, where the latter period falls right after a significant upgrade of the ENS (Lock et al. 2019). These choices enable us to investigate the effects of realistic initial condition and model improvements on the error growth curves. We decompose the ENS variance into variances at different scales by a normal mode decomposition (Žagar et al. 2015). This approach provides the global error growth curves that comprise errors at the different meridional and vertical scales (e.g., errors in the midlatitudes and the tropics for both the quasigeostrophic and inertio-gravity modes) for each zonal wavenumber k [for details, see Žagar et al. (2015)]. The error variance growth for

[1] Notice that β in Zetal2019 is normalized by E_{max}, the asymptotic value of the error E, which is one of the three parameters of the parametric error growth model, $dE/dt = (\alpha E + \beta)(1 - E/E_{max})$, of Dalcher and Kalnay (1987). Zetal2019 did not present their estimates of E_{max}, but the previous estimates for the ECMWF model at 500 hPa were well over 100 days (e.g., Magnusson and Kallen 2013). Notice also that E_{max} should be the same for the EDA and EDA0.1 experiments.

each value of k is fit by the parametric model of Žagar et al. (2017).[2] The hyperbolic-tangent structure of the parametric model fits both the early and late stages of the error growth well and the resulting estimates of the parameters can also be used to compute the α and β parameters of the model of Dalcher and Kalnay (1987).

Figure 1a shows the growth of the ENS variance for wavenumbers between $k = 5$ and $k = 100$. For each k, the estimate of the asymptotic value of the error variance $E_{\max}$ is used for the normalization of E to present the scale-dependent growth toward saturation. At the smaller scales shown in the figure, the errors are initially large compared to their saturation value and grow rapidly toward saturation. This behavior is reflected by the dominance of the β term of the Dalcher and Kalnay (1987) parametric model, which indicates a steep linear error growth. In contrast, at the larger scales (e.g., $k = 5$ and $k = 8$), the errors are initially small compared to their saturation values (around 1% of $E_{\max}$) and evolve in time by a multistage error growth process (e.g., Lorenz 2006; Tribbia and Baumhefner 2004; Simmons 2006).

In Fig. 1b, the forecast uncertainty growth of June 2018 (blue curves) is contrasted with that of May 2015 (black curves). For the sake of argument, we define the practical predictability limit by the forecast time at which the normalized variance is 0.6. The results suggest that the practical predictability time limit at the synoptic scales did not change much from May 2015 to June 2018: at zonal wavenumber 7, the characteristic scale of extratropical cyclones that dominate the day-to-day variability of the weather in the midlatitudes, the practical predictability limit was reached in 7.8 and 7.9 days in 2015 and 2018, respectively. This result is in a qualitative agreement with operational verification scores for the 500 hPa (Haiden et al. 2018). In contrast, the practical predictability improved significantly at the subsynoptic scales. For example, at $k = 35$, which corresponds to a zonal scale of $L = 2\pi R_e \cos(\phi)/(k/2) \approx 400$ km at 45°N, the practical predictability limit was reached in 1.9 days in May 2015 and in 2.7 days in June 2018. The improvement was even larger for $k = 65$ ($L \approx 220$ km at 45°N), for which the predictability limit more than doubled, from 0.6 days in May 2015 to about 1.4 days in June 2018. At the large scales, represented by $k = 4$ in the figure, the predictability limit is improved from 9.9 to 10.3 days. The better forecast skill at the subsynoptic scales and at large scales ($k \leq 4$) is likely to reflect model and initial-condition improvements between May 2015 and June 2018. Differences in the flow between the two periods may have also had some effect at the large scales.

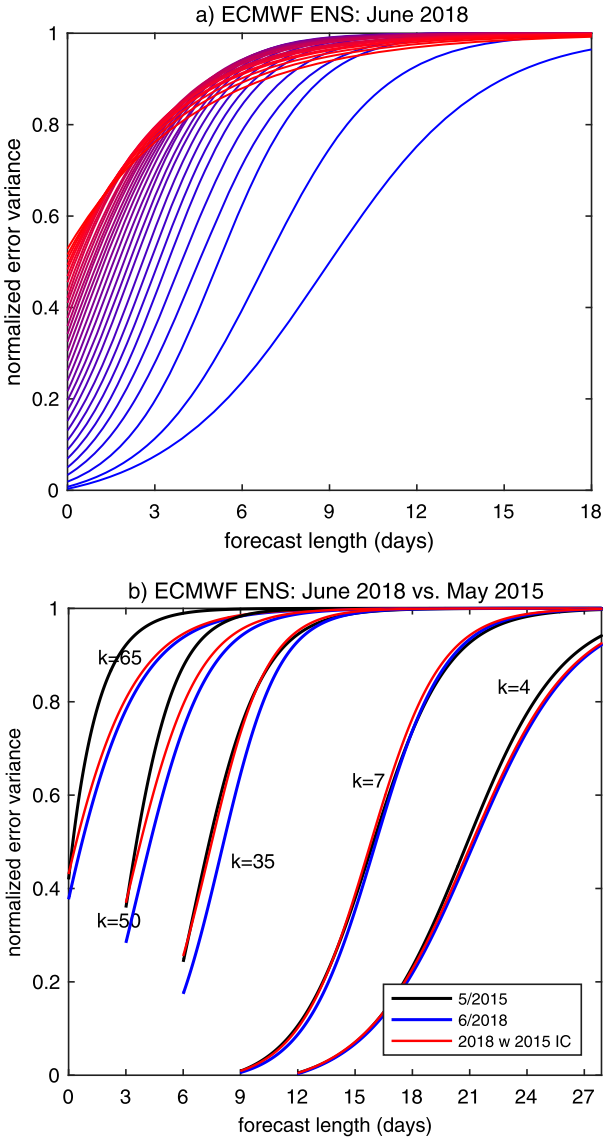

FIG. 1. Growth of the forecast uncertainty toward saturation in the operational ECMWF ENS. (a) The normalized ensemble variance at various zonal wavenumbers starting with $k = 5$ (bottom blue curve) up to $k = 100$ (top red curve), plotted every third wavenumber. (b) Comparison between the May 2015 (black lines) and June 2018 (blue lines) error growth curves at zonal wavenumbers $k = 4, 7, 35, 50$, and 65. The red lines correspond to the solution using the initial uncertainty from May 2015 and the parameters of the error growth curves from June 2018. The results for $k = 50, 35, 7$, and 4 are shifted by 3, 6, 9, and 12 days in the positive direction along the x axis, respectively, for transparency.

The uncertainty growth depends on the magnitude of the initial uncertainty and the parameters of the curves. The parameters for a specific wavenumber can change because of changes in the model errors and/or changes in the initial uncertainty at the other wavenumbers.

[2] We fit the ensemble variance, similar to Zetal2019, rather than the ensemble standard deviation as in Žagar et al. (2017).

To assess the relative importance of the reduction in the initial uncertainty versus the changes in the parameters of the curves in the reduction of the forecast uncertainty at the different wavenumbers between May 2015 and June 2018, we also show the hypothetical growth curves (red curves in Fig. 1b) that use the parameters for 2018, but with the initial values of the uncertainty from 2015. At wavenumbers $k = 7$ and $k = 35$, the hypothetical (red) curves are virtually identical to the (black) curve for 2015. This result indicates that the parameters of the curves at these wavenumbers changed little between 2015 and 2018. It also suggests that the improvement at $k = 35$ from 2015 to 2018 was probably the result of the reduction of the initial-condition uncertainty at that scale. In contrast, for smaller scales ($k = 50$ or $k = 65$), the red curves stay much closer to the (blue) curves for 2018 than to the (black) curves for 2015, suggesting that at these wavenumbers, the improvement was primarily the result of model improvements and/or initial-condition uncertainty reductions at other wavenumbers. While Fig. 1b shows results only for selected values of k, the results (not shown) do not change significantly if they are averaged over the synoptic, planetary and subsynoptic scales: little improvement at the synoptic scales, some improvement at the planetary scales and significant improvements at the subsynoptic scales.

Figure 2 compares the fitted curves of June 2018 with their hypothetical counterparts for a 75% (black curves) and a 99% (red curves) reduction of the initial ensemble variance. Based on the results shown in Fig. 1b, we can expect these hypothetical curves to provide a good prediction of the increase of predictability at wavenumbers $k = 7$ and $k = 35$. At $k = 7$, the gain of practical predictability would be 0.4–0.5 days for the 75% reduction of the initial uncertainty and about 0.6–0.7 days for the 99% reduction in the initial uncertainty. At wavenumber $k = 35$, the practical predictability limit would be reached in about 4.2 and 5.2 days for the 75% and 99% reduction, respectively, adding about 1.5 and 2.5 days of predictability.

Larger gains of predictability would be possible if the parameters of the error growth curves in Figs. 1 and 2 were changed by the reduction of model errors. For instance, improved modeling of the effects of highly localized processes (e.g., gravity wave drag) on the synoptic- and large-scale flow could potentially change the parameters of the curves. Such local effects can influence the larger-scale spectral distribution of the forecast uncertainty directly without an upscale cascade (Malardel and Wedi 2016). The upscale error growth could be represented more accurately by increasing model resolution. However, the upscale error growth is combined with the downscale propagation of the initial condition uncertainty at larger scales (e.g., Durran and Gingrich 2014) and the impact of model errors at all scales. In other words, making the perfect-model assumption as in Zetal2019 does not provide a reliable estimate of the predictability limit, as it ignores model errors by construction.

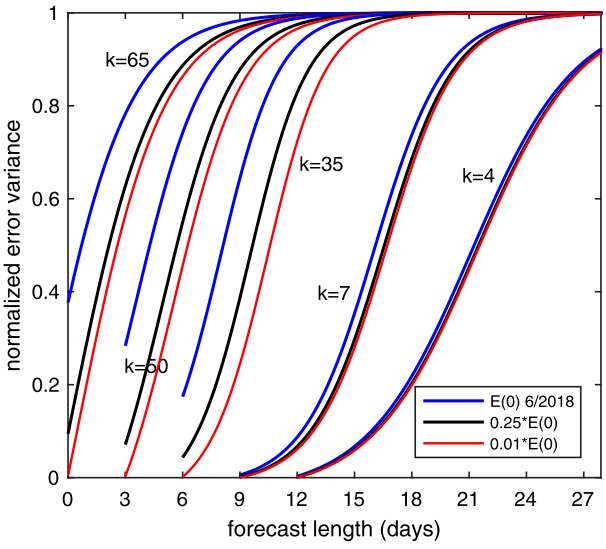

FIG. 2. Illustration of the effect of reducing the initial variance of the forecast errors on the error growth of June 2018 at zonal wavenumbers $k = 4$, 7, 35, 50, and 64. The black lines correspond to a 75% and the red lines to a 99% reduction of the initial variance. The results for $k = 50$, 35, 7, and 4 are shifted by 3, 6, 9, and 12 days in the positive direction along the x axis, respectively, for transparency.

4. Summary

In summary, we believe that the results of Zetal2019 do not justify their broad quantitative conclusion that reducing the analysis uncertainty alone could extend the midlatitude practical predictability from about 10 to 15 days. Our analysis of the uncertainty growth suggests that significant advancement of the practical predictability can be expected at the subsynoptic scales. However, these improvements are unlikely to lead to further considerable improvements of the predictability at the synoptic scales. A potential source of significant gains in practical predictability is further improvement of the predictions at the large (planetary) scales, where processes are heavily influenced by ocean–atmosphere, land–atmosphere and tropical–extratropical interactions. In a current-day state-of-the-science model, these interactions are simulated with considerable errors.

Acknowledgments. The ECMWF services available to the member states are gratefully acknowledged for the access to the ENS data on model levels. We are grateful to Jeffrey Anderson and Sergiy Vasylkevych for discussions and their comments on earlier drafts that helped improve the clarity of our arguments. Publication costs are contributed by the Cluster of Excellence ''CLICCS—Climate, Climatic Change, and Society,'' contribution to the Center for Earth System Research and Sustainability (CEN) of Universität Hamburg.

REFERENCES

Bonavita, M., L. Isaksen, and E. Holm, 2012: On the use of EDA background error variances in the ECMWF 4D-Var. *Quart. J. Roy. Meteor. Soc.*, **138**, 1540–1559, https://doi.org/10.1002/qj.1899.

Cardinali, C., N. Žagar, G. Radnoti, and R. Buizza, 2014: Representing model error in ensemble data assimilation. *Nonlinear Processes Geophys.*, **21**, 971–985, https://doi.org/10.5194/npg-21-971-2014.

Dalcher, A., and E. Kalnay, 1987: Error growth and predictability in operational ECMWF forecasts. *Tellus*, **39A**, 474–491, https://doi.org/10.1111/j.1600-0870.1987.tb00322.x.

Durran, D. R., and M. Gingrich, 2014: Atmospheric predictability: Why butterflies are not of practical importance. *J. Atmos. Sci.*, **71**, 2476–2488, https://doi.org/10.1175/JAS-D-14-0007.1.

Haiden, T., and Coauthors, 2018: Evaluation of ECMWF forecasts, including the 2018 upgrade. ECMWF Tech. Memo. 831, 52 pp., https://www.ecmwf.int/node/18746.

Harlim, J., M. Oczkowski, J. A. Yorke, E. Kalnay, and B. R. Hunt, 2005: Convex error growth patterns in a global weather model. *Phys. Rev. Lett.*, **94**, 228501, https://doi.org/10.1103/PHYSREVLETT.94.228501.

Herrera, M. A., I. Szunyogh, and J. Tribbia, 2016: Forecast uncertainty dynamics in the THORPEX Interactive Grand Global Ensemble (TIGGE). *Mon. Wea. Rev.*, **144**, 2739–2766, https://doi.org/10.1175/MWR-D-15-0293.1.

Hoskins, B. J., R. Buizza, and J. Badger, 2000: The nature of singular vector growth and structure. *Quart. J. Roy. Meteor. Soc.*, **126**, 1565–1580, https://doi.org/10.1002/qj.49712656601.

Isaksen, L., M. Bonavita, R. Buizza, M. Fisher, J. Haseler, M. Leutbecher, and L. Raynaud, 2010: Ensemble of data assimilations at ECMWF. ECMWF Tech. Memo. 636, 41 pp., https://www.ecmwf.int/node/10125.

Leutbecher, M., and Coauthors, 2017: Stochastic representations of model uncertainties at ECMWF: State of the art and future vision. *Quart. J. Roy. Meteor. Soc.*, **143**, 2315–2339, https://doi.org/10.1002/qj.3094.

Lock, S.-J., S. Lang, M. Leutbecher, R. Hogan, and F. Vitart, 2019: Stochastically perturbed parametrization tendencies (SPPT) scheme and associated revisions in the ECMWF ensembles. *Quart. J. Roy. Meteor. Soc.*, **145**, 75–89, https://doi.org/10.1002/qj.3570.

Loeser, C. F., M. A. Herrera, and I. Szunyogh, 2017: An assessment of the performance of the operational global ensemble forecast systems in predicting the forecast uncertainty. *Wea. Forecasting*, **32**, 149–164, https://doi.org/10.1175/WAF-D-16-0126.1.

Lorenz, E. N., 2006: Predictability—A problem partly solved. *Predictability of Weather and Climate*, T. Palmer and R. Hagedorn, Eds., Cambridge University Press, 40–58.

Magnusson, L., and E. Kallen, 2013: Factors influencing skill improvements in the ECMWF forecasting system. *Mon. Wea. Rev.*, **141**, 3142–3153, https://doi.org/10.1175/MWR-D-12-00318.1.

Malardel, S., and N. P. Wedi, 2016: How does subgrid-scale parametrization influence nonlinear spectral energy fluxes in global NWP models? *J. Geophys. Res. Atmos.*, **121**, 5395–5410, https://doi.org/10.1002/2015JD023970.

Simmons, A., 2006: Observations, assimilation and the improvement of global weather prediction—Some results from operational forecasting and ERA-40. *Predictability of Weather and Climate*, T. Palmer and R. Hagedorn, Eds., Cambridge University Press, 428–458.

——, and A. Hollingsworth, 2002: Some aspects of the improvement in skill of numerical weather prediction. *Quart. J. Roy. Meteor. Soc.*, **128**, 647–677, https://doi.org/10.1256/003590002321042135.

Tribbia, J., and D. P. Baumhefner, 2004: Scale interactions and atmospheric predictability: An updated perspective. *Mon. Wea. Rev.*, **132**, 703–713, https://doi.org/10.1175/1520-0493(2004)132<0703:SIAAPA>2.0.CO;2.

Žagar, N., 2017: A global perspective of the limits of prediction skill of NWP models. *Tellus*, **69A**, 1317573, https://doi.org/10.1080/16000870.2017.1317573.

——, L. Isaksen, D. Tan, and J. Tribbia, 2013: Balance properties of the short-range forecast errors in the ECMWF 4D-Var ensemble. *Quart. J. Roy. Meteor. Soc.*, **139**, 1229–1238, https://doi.org/10.1002/qj.2033.

——, R. Buizza, and J. Tribbia, 2015: A three-dimensional multivariate modal analysis of atmospheric predictability with application to the ECMWF ensemble. *J. Atmos. Sci.*, **72**, 4423–4444, https://doi.org/10.1175/JAS-D-15-0061.1.

——, M. Horvat, Ž. Zaplotnik, and L. Magnusson, 2017: Scale-dependent estimates of the growth of forecast uncertainties in a global prediction system. *Tellus*, **69A**, 1287492, https://doi.org/10.1080/16000870.2017.1287492.

Zhang, F., Y. Q. Sun, L. Magnusson, R. Buizza, S.-J. Lin, J.-H. Chen, and K. Emanuel, 2019: What is the predictability limit of midlatitude weather? *J. Atmos. Sci.*, **76**, 1077–1091, https://doi.org/10.1175/JAS-D-18-0269.1.